Available online at www.sciencedirect.com
ScienceDirect
Solid State Communications 143 (2007) 250–254
solid state communications
www.elsevier.com/locate/ssc

Improved optical and structural properties of ZnO thin films by rapid thermal annealing

Yueh-Chien Lee[a,*], Sheng-Yao Hu[b], Walter Water[c], Ying-Sheng Huang[d], Min-De Yang[e], Ji-Lin Shen[e], Kwong-Kau Tiong[f], Chia-Chih Huang[a]

[a] *Department of Electronic Engineering, Tung Nan Institute of Technology, Taipei, Taiwan, ROC*
[b] *Department of Electrical Engineering, Tung Fang Institute of Technology, Hunei Township, Kaohsiung County, Taiwan, ROC*
[c] *Department of Electronic Engineering, National Formosa University, Yunlin, Taiwan, ROC*
[d] *Department of Electronic Engineering, National Taiwan University of Science and Technology, Taipei, Taiwan, ROC*
[e] *Department of Physics, Chung Yuan Christian University, Chung-Li, Taiwan, ROC*
[f] *Department of Electrical Engineering, National Taiwan Ocean University, Keelung, Taiwan, ROC*

Received 26 February 2007; received in revised form 6 May 2007; accepted 13 May 2007 by E.G. Wang
Available online 26 May 2007

Abstract

The influence of rapid thermal annealing (RTA) on the optical and structural properties of ZnO thin films grown on Si substrate has been investigated by X-ray diffraction (XRD), photoluminescence (PL), and Raman scattering (RS) measurements. The relaxation of the residual stress by increasing the annealing temperature during the RTA process was observed by the measured shift of (002) XRD diffraction peak towards 34.40° and the shift of RS E_2 (high) mode closer to 437 cm^{-1}. The process also resulted in a reduction of the measured full-width at half maximum (FWHM) of the PL emission line and that of the asymmetrical broadening of RS E_2 (high) mode. The observed changes have demonstrated that RTA is a viable technique for improving the crystalline quality of ZnO/Si films.

PACS: 63.20.-e; 78.30.-j; 78.30.Fs

Keywords: A. Semiconductors; D. Optical properties

1. Introduction

Zinc Oxide (ZnO) is a II–VI compound semiconductor crystallizes in hexagonal wurtzite structure with a large exciton binding energy (∼60 meV) and provides efficient excitonic emissions at room temperature. Moreover, ZnO with a wide-band-gap of 3.37 eV at room temperature has attracted considerable attention as a versatile material for optoelectronic applications such as sensors [1], surface acoustic wave devices [2], light emitting diodes and laser diodes [3,4]. However, the crystal quality of ZnO thin films strongly depends on the growth techniques, growth conditions and selected substrates. Numerous researchers have attempted to grow the high crystalline of ZnO films deposited on Si substrates because of the lower cost and larger wafer size [5]. However, the large lattice mismatch and large difference in the thermal expansion coefficients between ZnO films and Si substrates have resulted in a built-in residual stress to exist in the deposited ZnO films. Therefore, it is a challenge to obtain high crystal quality ZnO thin films deposited on Si substrates (ZnO/Si).

In order to grow high quality ZnO/Si films, several deposition techniques such as sputtering [2,3], molecular beam deposition (MBE) [4,6], chemical vapour deposition (CVD) [5,7] and pulsed laser deposition (PLD) [8] have been discussed. Among the different deposition techniques, the rf sputtering is the most commonly used technique due to its simple set-up, high deposition rate and low substrate temperature. However, in order to obtain high quality ZnO/Si films by rf sputtering technique it is necessary to have optimal control of deposition conditions such as working pressure, substrate temperature, deposition power and growth ambient [2,3]. On

* Corresponding author. Tel.: +886 2 8662 5856x533; fax: +886 2 2664 4079.
E-mail address: jacklee@mail.tnit.edu.tw (Y.-C. Lee).

0038-1098/$ - see front matter © 2007 Elsevier Ltd. All rights reserved.
doi:10.1016/j.ssc.2007.05.021

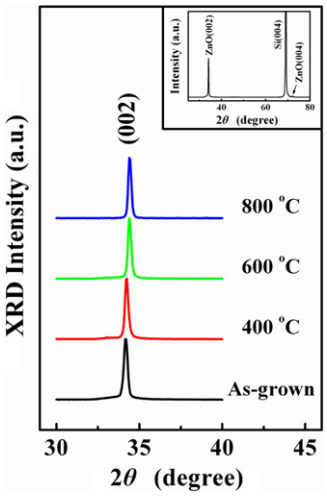

Fig. 1. X-ray diffraction measurements of the as-grown and annealed ZnO/Si films. The inset is the typical XRD spectrum scanned for the as-grown ZnO/Si film.

the other hand, the temperature annealing treatment is widely known as a conventional and effective technique to improve the crystalline quality. Hong et al. [9] and Jung et al. [10] have investigated the annealing effects on the characteristics of sputtered ZnO/Si films and suggested that higher annealing temperature could improve crystallinity more effectively. The thermal annealing process for the sputtered ZnO/Si films could further be improved using the rapid thermal annealing (RTA) technique [11]. The annealing period of RTA treatment is shorter than that of traditional annealing with furnace. Hence, controlling the details of RTA is worth the effort to explore the potential of such technique for improving the electrical and optical properties of semiconductor materials [11].

In this work, the influence of rapid thermal annealing on structural and optical properties of ZnO films was analysed by X-ray diffraction (XRD), photoluminescence (PL), and Raman scattering (RS) techniques. For the XRD, the measured shift of the (002) diffraction peak with reference to the ideal single crystal ((002) diffraction peak at 34.40° has been used an indicator of the crystalline quality of the ZnO/Si thin films. The temperature dependence of the full-width at half-maximum (FWHM) of near-band-edge (NBE) emission of PL spectra has been studied. The FWHM of NBE emission is directly related with the crystal quality of ZnO/Si films. In addition, RS was used to analyse the variation of microscopic crystalline structure of ZnO/Si thin films with the annealing temperature. The linewidth and asymmetrical broadening of the RS E_2 (high) mode were evaluated via the spatial correlation (SC) model [12].

2. Experiment

ZnO films were deposited by rf magnetron sputtering system using a ZnO target (99.9%). The substrate is p-type silicon with (100) orientation. Si substrates were thoroughly cleaned with organic solvents and dried before loading in the sputtering system. The chamber was pumped down to 1.5×10^{-5} Torr using a diffusion pump before introducing the premixed Ar and O_2 sputtering gases. Throughout all experiments, the target was presputtered for 15 min under 150 W rf power before the actual deposition began, in order to remove any contamination on the target surface and make the system stable and reach optimum condition. In the actual sputtering, the sputtering power is controlled at 100 W, the sputtering pressure is 1.33 N/m^2, ratio of O_2/Ar is 0.75, distance between substrate and target is 50 mm, and the substrate is not heated. Then the as-grown ZnO/Si sample was divided into four pieces, three of which were undergone the RTA processes. The samples were annealed under a constant oxygen flow rate of 500 sccm for 30 s at 400, 600, and 800 °C, respectively.

The XRD patterns of the ZnO films were obtained using Cu Kα radiation. The PL measurements were performed in air at room temperature. A focused diode-pumped laser (266 nm) with a power density of 5 mW/cm^2 was used as an excitation source. The luminescence was collected using a spectrometer (Jobin Yvon 550) with a grating with 1200 grooves/mm, and detected using a cooled GaAs photomultiplier tube. The Raman scattering measurements were carried out using the Renishaw System (inVia Raman microscope) at room temperature. Raman spectra were excited with the 514.5 nm line of an Ar^+ laser at an incident power of 10 mW.

3. Results and discussion

A typical XRD spectrum scanned from 20°(2θ) to 80° continuously for the as-grown ZnO film is depicted in the inset of Fig. 1. Only the ZnO(002) and ZnO(004) XRD lines are present along with the (004) line of the Si substrate. The sharp diffraction peaks of ZnO(002) and ZnO(004) indicate that the ZnO film is highly c-axis oriented [13,14]. The (002) diffraction peak for the as-grown, RTA at $T = 400$ °C, 600 °C, and 800 °C ZnO/Si films shown in Fig. 1 are observed at $2\theta = 34.18°, 34.22°, 34.38°$, and 34.39°, respectively. The shift of the (002) diffraction peak by 0.22 for the as-grown with respect to the reference strain-free ZnO film (34.40°) showed the existence of residual compressive stress between ZnO and the Si substrate [2,3,11]. The compressive stress can be relaxed almost completely through high temperature RTA process at 800 °C. The fitted values of FWHM of (002) peak of the as-grown and annealed ZnO/Si films are also listed in Table 1. The FWHM for the as-grown sample was fitted to be 0.236° and decreased to 0.188° for the sample annealed at 800 °C.

The origin of the residual stress in the as-grown ZnO/Si film can be understood as follows: it is known that the residual stress in ZnO films contains a thermal stress component and an intrinsic stress component [2,15]. The thermal stress is due to the difference in the thermal expansion coefficient between ZnO (4.75×10^{-6}/K) and silicon substrate (2.6×10^{-6}/K) [16]. Since the thermal expansion coefficient of ZnO is bigger than that of silicon substrate, the substrate gives a resultant tensile stress effect to the ZnO film as the substrate cools down from high temperature to room temperature. Intrinsic stress has its origin in the imperfection of the crystallites during growth. Several growth parameters, such as deposition temperature, deposition pressure, deposition power, and gas

Table 1
The FWHM of XRD and PL and the values of asymmetrical ratio (Γ_a/Γ_b) and correlation length (L) for the E_2 (high) phonon mode of ZnO/Si films following rapid thermal annealing

RTA temperature	XRD	PL		Raman	
	FWHM (degree)	FWHM (meV)		(Γ_a/Γ_b)	L(Å)
		12 K	300 K		
As-grown	0.236 ± 0.006	111 ± 3	224 ± 5	1.49 ± 0.02	67 ± 2
400 °C	0.220 ± 0.006	93 ± 3	173 ± 5	1.31 ± 0.02	72 ± 2
600 °C	0.204 ± 0.004	84 ± 2	155 ± 3	1.23 ± 0.02	77 ± 2
800 °C	0.188 ± 0.004	82 ± 2	129 ± 3	1.20 ± 0.02	80 ± 2

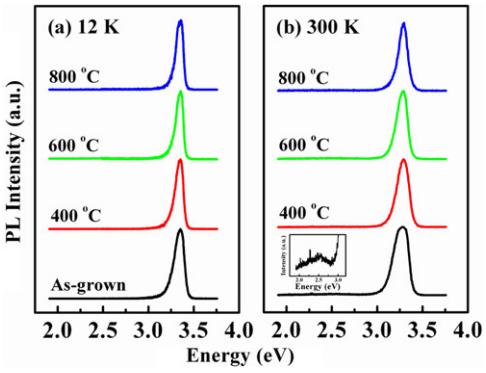

Fig. 2. (a) 12 K and (b) 300 K photoluminescence spectra of ZnO/Si films following annealing. The inset shows the visible emission of 300 K PL of the as-grown ZnO film (the bottom of (b)).

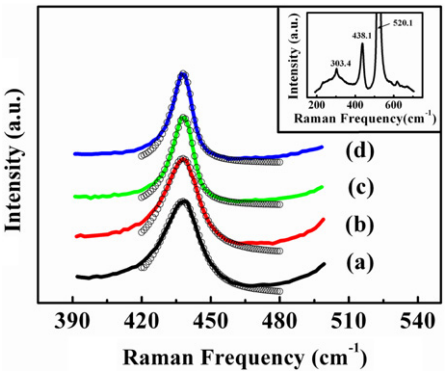

Fig. 3. Experimental line shapes of the E_2 (high) phonon mode of ZnO/Si films with (a) as-grown, (b) annealed at 400 °C, (c) annealed at 600 °C, and (d) annealed at 800 °C. The inset is the typical Raman spectrum of the as-grown ZnO/Si film taken at room temperature.

mixture would contribute to the intrinsic stress. The intrinsic stress in ZnO should be compressive and its magnitude is larger than the (tensile) thermal stress component, resulting in an overall residual compressive stress in the as-grown ZnO films [2,15].

Fig. 2(a) and (b) display the 12 and 300 K PL spectra of ZnO/Si films following RTA with different annealing temperature. For the as-grown ZnO/Si sample, the prominent PL emission line is located at 3.35 eV at 12 K and 3.28 eV at 300 K. The prominent PL signal has been known as the UV near-band-edge (NBE) transition [3–5,11]. On the other hand, as shown in the inset of Fig. 2(b), the 300 K PL spectrum of the as-grown ZnO/Si exhibits a very weak green emission centered approximately at 2.5 eV. The weak signal is commonly regarded as the defect level of oxygen vacancies [5, 7]. For the RTA-treated samples, the intensity of the weak green emission line diminishes even further and becomes not observable. Hur et al. [17] and Zhao et al. [18] have reported the formations of ZnO films annealed under O_2 ambient and indicated that sufficient amount of oxygen diffusing into the sample should decrease the concentration of oxygen vacancies in ZnO films and resulting in a decrease of the deep level emission. This reasoning is well correlated to our present experimental observation of the absence of deep level signal in the RTA-treated samples. The fitted FWHM of PL peak of as-grown ZnO film is about 111 meV at 12 K and is about 224 meV at 300 K. The FWHM of PL signal as a function of annealing temperature is listed in the Table 1 and showed significant decrease with increasing annealing temperature. The sample annealed at 800 °C exhibits the lowest value of FWHM ~82 (129 meV) meV at 12 K (300 K). It is known that the PL linewidth is directly related to the crystal quality of the sample, in which a narrower PL linewidth is regarded as a clear evidence for the improvement of crystal quality [9,10]. The observed change showed the potential worth of RTA technique for the improvement of crystal quality of the ZnO/Si thin films.

In order to understand the effects of annealing temperature of RTA, the RS was carried out to study the microscopic nature of structural and/or topological disorder of ZnO/Si thin films. The peak position of Raman signal can be utilized to investigate the variation of the residual stress within ZnO/Si films after RTA. Further, the line shape of Raman signal also provides more information relating to the structural imperfections [12, 19]. The inset of Fig. 3 shows a typical Raman spectrum of the as-grown ZnO thin film taken at room temperature. The two peaks observed at 303.4 and 520.1 cm^{-1} were attributed to the optical phonon mode of Si substrate [20]. The peak at 438.1 cm^{-1} was attributed to the lattice vibration mode of E_2 (high) of the ZnO sample [20,21].

Huang et al. have demonstrated that the stress induced in crystal would obviously affect the E_2 (high) phonon frequency in the hexagonal wurtzite structure crystals [21]. Hence a thorough investigation of the RS E_2 (high) mode should yield useful information of the residual stress in the as-grown and RTA-treated ZnO/Si thin films. The upshift of E_2 (high) mode is correlated with the presence of compressive stress, while the E_2 (high) mode downshift is related with tensile stress [13, 21]. As shown in Fig. 3, the E_2 (high) phonon frequency shifts from 438.1 cm^{-1} for the as-grown ZnO film to 437.4 cm^{-1}

for the sample annealed at 800 °C. The peak position of E_2 (high) shifting close to 437 cm^{-1} (single crystal) implies that the compressive stress would be relaxed with RTA, which is in agreement with the result of XRD.

In addition, the linewidth and asymmetry of the Raman spectra were analyzed to study the nature of structural disorder in ZnO/Si thin films. The linewidth broadening of Raman line shapes are sensitive to the variations of residual stress within ZnO/Si films. The Raman peak in Fig. 3 shows an asymmetrical line shape, which can be described by the spatial correlation (SC) model [12]. According to the SC model, the spatial correlation function of the phonon for a pure compound semiconductor is infinite and the phonon eigenstates are plane waves. These lead to the usual $q = 0$ momentum selection rule of Raman scattering and the Raman spectrum shows a symmetric Lorentzian profile ($\Gamma_a = \Gamma_b$, where Γ_a (Γ_b) represents the low-energy (high-energy) half width of half maximum). The alloying or any imperfection in semiconductors may destroy the configurational symmetry and break down the $q = 0$ momentum selection rule. The spatial correlation function of phonon hence becomes finite. The finite phonon mode will lead to the broadening and asymmetrical ($\Gamma_a > \Gamma_b$) of the Raman line shape.

Based on the SC model, the Gaussian spatial correlation function $\exp(-2r^2/L^2)$, where L is the phonon correlation length, has been successfully used to account for q-vector relaxation related to finite-size effects and structural disorder. Then, the Raman intensity $I(\omega)$ at a frequency ω can be written as

$$I(\omega) \propto \int \frac{\exp\left(-q^2L^2/4\right)}{[\omega - \omega(q)]^2 + (\Gamma_0/2)^2} \mathrm{d}^3q \tag{1}$$

where q is the reduced wave vector in the unit of $2\pi/a$, a is the lattice constant, and Γ_0 ($\approx$5.05 cm^{-1}) is the intrinsic linewidth of E_2 (high) phonon mode [22]. Here we consider that the Gaussian distribution is associated with the finite size of thin film region [23] and rewrite the Eq. (1) as

$$I(\omega) \propto \int \frac{\exp\left(-q^2L^2/16\pi^2\right)}{[\omega - \omega(q)]^2 + (\Gamma_0/2)^2} \mathrm{d}^3q. \tag{2}$$

For the dispersion $\omega(q)$, we take the analytic model relationship [24]:

$$\omega(q) = A + B\cos(\pi q) \tag{3}$$

where $A = 424.5$ cm^{-1} and $B = 12.5$ cm^{-1} for the E_2 (high) phonon dispersion according to the *ab initio* phonon-dispersion relations calculated for ZnO. [19,25]. Eqs. (2) and (3) shows that if L is finite, the q selection rule may relax, and additional transitions by phonon with lower energy at $q \neq 0$ may occur, which lead to the broadening and asymmetry of the Raman line shape. The opened circles in Fig. 3 exhibit the calculated results with SC model, which are in good agreement with experimental data. The values of the correlation length L and the asymmetrical ratio (Γ_a/Γ_b) can be evaluated from the Raman line shape fitting and are listed in the Table 1. It is found that the correlation length L increases and the asymmetrical ratio (Γ_a/Γ_b) decreases with increasing annealing temperature.

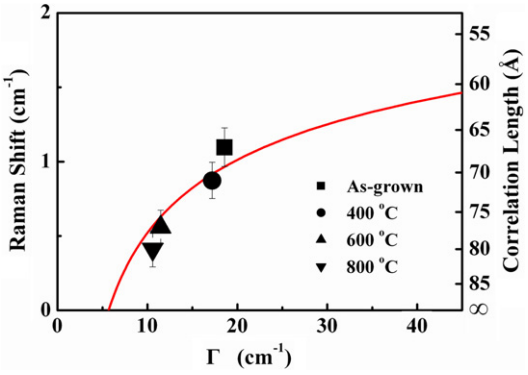

Fig. 4. Relationship between Raman shift and broadening Γ as a function of correlation length L for ZnO/Si films following annealing.

Fig. 4 shows the Raman shift from 437 cm^{-1} and the broadening Γ of E_2 (high) phonon as a function of correlation length L as determined from Eqs. (2) and (3) plotted by the solid line. It is shown that the agreements between the experimental and calculated linewidth and shift of E_2 (high) signal are reasonable. In the case of a single crystal with very low non-stoichiometry, the correlation length will tend towards infinity. Kosacki et al. [26] and Chen et al. [27] have reported that the correlation length should not only be related to the grain size but also to the structural damage or the distance between the defects/impurities, such as oxygen vacancies [26]. In this study, the correlation length was discussed as a fitting parameter to investigate the localized region of E_2 (high) phonon [28]. The value of L increases with increasing annealing temperature, which indicates that the phonon extended region becomes larger due to the improvement of crystal quality of ZnO/Si films. Hence we have demonstrated experimentally that higher annealing temperature can reduce the residual stress between ZnO film and Si substrate resulting in improvement of the crystal quality.

4. Conclusion

In summary, we report the XRD, PL, and RS of the as-grown and RTA-treated ZnO/Si films. The FWHM of NBE emission of PL could be decreased by increasing annealing temperature. The shift of the peak position of (002) XRD diffraction line and that of RS E_2 (high) phonon mode show that the residual compressive stress can be reduced after annealing. The beneficial effect of thermal annealing has been shown to be more pronounced for higher temperature annealing. Additionally, the RS line shapes for the E_2 (high) phonon mode of ZnO films are well described by SC model. The asymmetrical ratio and linewidth of Raman spectra decreases with increasing annealing temperature. The results demonstrated the potential of the RTA treatment as a viable technique for improving the crystal quality of ZnO thin films.

Acknowledgements

The author Y.C. Lee would like to acknowledge the support of the National Science Council Project No. NSC 95-2112-M-236-002. S.Y. Hu acknowledges the support of the National Science Council Project No. NSC95-2745-M-272-001.

References

[1] J.E. Nause, III-Vs Rev. 12 (1999) 28.
[2] W. Water, S.Y. Chu, Mater. Lett. 55 (2002) 67.
[3] T. Shimomura, D. Kim, M. Nakayama, J. Lumin. 112 (2005) 191.
[4] M.J.H. Henseler, W.C.T. Lee, P. Miller, S.M. Durbin, R.J. Reeves, J. Crystal Growth 287 (2006) 48.
[5] K. Haga, T. Suzuki, Y. Kashiwaba, H. Watanabe, B.P. Zhang, Y. Segawa, Thin Solid Films 433 (2003) 131.
[6] X.N. Wang, Y. Wang, Z.X. Mei, J. Dong, Z.Q. Zeng, H.T. Yuan, T.C. Zhang, X.L. Du, J.F. Jia, Q.K. Xue, X.N. Zhang, Z. Zhang, Z.F. Li, W. Lu, Appl. Phys. Lett. 90 (2007) 151912.
[7] J.D. Ye, S.L. Gu, S.M. Zhu, F. Qin, S.M. Liu, W. Liu, X. Zhou, L.Q. Hu, R. Zhang, Y. Shi, Y.D. Zheng, J. Appl. Phys. 96 (2004) 5308.
[8] H.S. Kang, J.S. Kang, S.S. Pang, E.S. Shim, S.Y. Lee, Mater. Sci. Eng. B 102 (2003) 313.
[9] R. Hong, J. Huang, H. He, Z. Fan, J. Shao, Appl. Surf. Sci. 242 (2005) 346.
[10] M. Jung, J. Lee, S. Park, H. Kim, J. Chang, J. Crystal Growth 283 (2005) 384.
[11] K.K. Kim, S. Niki, J.Y. Oh, J.O. Song, T.Y. Seong, S.J. Park, S. Fujita, S.W. Kim, J. Appl. Phys. 97 (2005) 066103.
[12] P. Parayanthal, F.H. Pollak, Phys. Rev. Lett. 52 (1984) 1822.
[13] W.J. Shen, J. Wang, Q.Y. Wang, Y. Duan, Y.P. Zeng, J. Phys. D: Appl. Phys. 39 (2006) 269.
[14] Y.F. Lu, H.Q. Ni, Z.H. Mai, Z.M. Ren, J. Appl. Phys. 88 (2000) 498.
[15] A. Cimpoiasu, N.M. van der Pers, Th.H. de Keyser, A. Venema, M.J. Vellekoop, Smart Mater. Struct. 5 (1996) 744.
[16] L. Wang, Y. Pu, Y.F. Chen, C.L. Mo, W.Q. Fang, C.B. Xiong, J.N. Dai, F.Y. Jiang, J. Crystal Growth 284 (2005) 459.
[17] T.B. Hur, G.S. Jeen, Y.H. Hwang, H.K. Kim, J. Appl. Phys. 94 (2003) 5787.
[18] Q. Zhao, X.Y. Xu, X.F. Song, X.Z. Zhang, D.P. Yu, C.P. Li, L. Guo, Appl. Phys. Lett. 88 (2006) 033102.
[19] J.B. Wang, H.M. Zhong, Z.F. Li, W. Lu, J. Appl. Phys. 97 (2005) 086105.
[20] H.Z. Wu, K.M. He, D.J. Qiu, D.M. Huang, J. Crystal Growth 217 (2000) 131.
[21] Y. Huang, M. Liu, Z. Li, Y. Zeng, S. Liu, Mater. Sci. Eng. B 97 (2003) 111.
[22] J. Serrano, F.J. Manjón, A.H. Romero, F. Widulle, R. Lauck, M. Cardona, Phys. Rev. Lett. 90 (2003) 055510.
[23] I.H. Campbell, P.M. Fauchet, Solid State Commun. 58 (1986) 739.
[24] K.K. Tiong, P.M. Amirtharaj, F.H. Pollak, D.E. Aspnes, Appl. Phys. Lett. 44 (1984) 122.
[25] J. Serrano, F. Widulle, A.H. Romero, A. Rubio, R. Lauck, M. Cardona, Phys. Status Solidi B 235 (2003) 260.
[26] I. Kosacki, T. Suzuki, H.U. Anderson, P. Colomban, Solid State Ionics 149 (2002) 99.
[27] R.S. Chen, C.C. Chen, Y.S. Huang, C.T. Chia, H.P. Chen, D.S. Tsai, K.K. Tiong, Solid State Commun. 131 (2004) 349.
[28] L.Y. Lin, C.W. Chang, W.H. Chen, Phys. Rev. B 69 (2004) 075204.